G-Quadruplexes

Deutsche Ausgabe: DOI: 10.1002/ange.201510269
Internationale Ausgabe: DOI: 10.1002/anie.201510269

Photoresponsive Formation of an Intermolecular Minimal G-Quadruplex Motif

Julie Thevarpadam[+], Irene Bessi[+], Oliver Binas[+], Diana P. N. Gonçalves, Chavdar Slavov, Hendrik R. A. Jonker, Christian Richter, Josef Wachtveitl, Harald Schwalbe, and Alexander Heckel**

In memory of Gerhard Quinkert

Abstract: *The ability of three different bifunctional azobenzene linkers to enable the photoreversible formation of a defined intermolecular two-tetrad G-quadruplex upon UV/Vis irradiation was investigated. Circular dichroism and NMR spectroscopic data showed the formation of G-quadruplexes with K^+ ions at room temperature in all three cases with the corresponding azobenzene linker in an E conformation. However, only the para–para-substituted azobenzene derivative enables photoswitching between a nonpolymorphic, stacked, tetramolecular G-quadruplex and an unstructured state after E–Z isomerization.*

G-Quadruplexes are important DNA secondary structures. The structures form in an intramolecular manner or by association of multiple strands and can exist in many polymorphic forms.[1–4] G-Quadruplexes are important regulatory elements in the genome[5,6] but they are also selected in SELEX procedures as versatile aptamers (SELEX = systematic enrichment of ligands by exponential amplification).[7] For example a simple G-rich DNA 15mer can inhibit blood clotting.[8] In DNA nanoarchitectures, G-quadruplexes can act as interesting structural scaffolds.[9–14]

Light is an ideal external trigger signal that can be highly selective and superior to changes in temperature and pH value. Localized irradiation, for example in laser scanning microscopes, allows for very precise spatiotemporal and dose control,[15–18] far beyond the precision of the injection of trigger compounds, as recently shown for blood clotting and miRNA.[19,20]

The ability to control a process by light can be introduced either by using photolabile groups or photoswitches such as azobenzene.[24,25] The use of photolabile groups has been applied to G-quadruplexes which were either formed or destroyed irreversibly upon light irradiation.[21–23]

In the G-quadruplex field, Ogasawara and Maeda have used stilbene-type substituents to control the formation of G-quadruplexes by light-induced *E–Z* isomerization.[26] Spada et al. controlled the self-assembly of guanosine monomers in a similar fashion.[27] The formation of G-quadruplexes can also be induced by small molecules that act as molecular chaperons in the absence of cations.[28–30] Zhou et al. developed azobenzene-containing small-molecule chaperones to regulate G-quadruplex formation.[31] Tan et al. synthesized an azobenzene-modified antisense DNA linked to a thrombin-binding aptamer to regulate G-quadruplex formation.[32]

Herein, we present a minimal light-switchable DNA module enabling the formation of an intermolecular and conformationally well-defined G-quadruplex structure with a photoswitchable azobenzene residue as part of the backbone structure (Figure 1).

Azobenzene derivatives **Az1**, **Az2**, and **Az3** (Figure 2a) were employed as photoswitchable linkers between two sets of two consecutive guanosine moieties and were introduced using DNA solid-phase synthesis. The size and substitution patterns on the azo linkers were chosen to offer a suitable balance between the rigidity and flexibility of the overall structure, such that the photoswitch in the *E* conformation should permit the formation of a G-quadruplex, whereas in the *Z* conformation no such G-quadruplex formation should be possible. Simple predictions suggested that **Az1** can bridge a distance of 13.2–13.6 Å in the *E* conformation and 7.7–

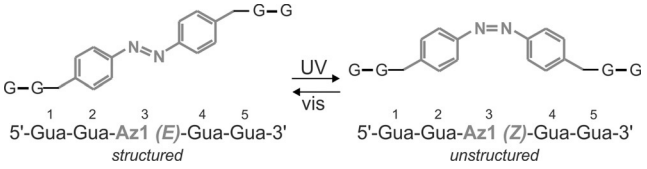

Figure 1. Sequence and numbering of the azobenzene derivative used and characterized in this study, with the azo unit (**Az1**) shown in gray.

[*] J. Thevarpadam,[+] Dr. D. P. N. Gonçalves, Prof. Dr. A. Heckel
Goethe University Frankfurt
Institute for Organic Chemistry and Chemical Biology
Buchmann Institute for Molecular Life Sciences
Max-von-Laue-Strasse 9, 60438 Frankfurt (Germany)
E-mail: heckel@uni-frankfurt.de
Homepage: http://photochem.uni-frankfurt.de
I. Bessi,[+] O. Binas,[+] Dr. H. R. A. Jonker, Dr. C. Richter, Prof. Dr. H. Schwalbe
Institute for Organic Chemistry and Chemical Biology
Center for Biomolecular Magnetic Resonance (BMRZ)
Max-von-Laue-Strasse 9, 60438 Frankfurt (Germany)
E-mail: schwalbe@nmr.uni-frankfurt.de
Homepage: http://schwalbe.org.chemie.uni-frankfurt.de
Dr. C. Slavov, Prof. Dr. J. Wachtveitl
Institute for Physical and Theoretical Chemistry
Max-von-Laue-Strasse 7, 60438 Frankfurt (Germany)
[+] These authors contributed equally to this work.

Supporting information for this article is available on the WWW under http://dx.doi.org/10.1002/anie.201510269.

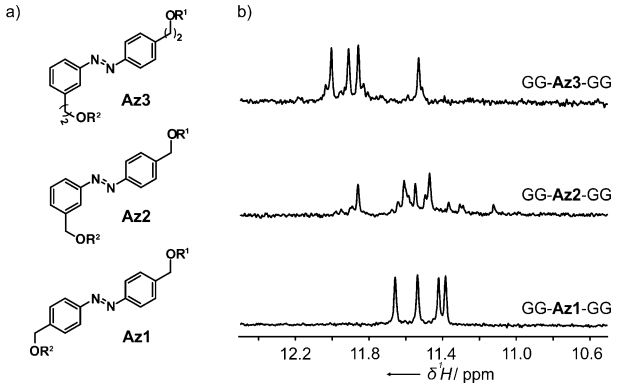

Figure 2. a) The structures of the azo units employed in this study. b) Imino regions of the 1D ^{1}H NMR spectra of GG-**Az1**-GG, GG-**Az2**-GG, and GG-**Az3**-GG in the presence of KCl (100 mM). Experimental conditions: DNA (50 μM), Tris-HCl buffer (50 mM; pH 7.4), 298 K, 600 MHz.

11.5 Å in the *Z* conformation between the two oxygen atoms adjacent to the azobenzene core. Going from a *para–para* to a *para–meta* substitution pattern in **Az2**, these values change to 11.1–13.6 Å and 9.0–11.9 Å, respectively. The O···O distance at equivalent positions in the narrow grooves in G-quadruplex structures can reach 11–12 Å (see for example PDB 2GKU). We also included the double homologue **Az3** (8.8–14 Å in the *E* conformation and 7.3–12.4 Å in the *Z* conformation). Clearly, minor changes in the structure of the azo linker result in significant changes of the "hinge qualities" of the photoswitch linkers. All of these considerations should be considered with reservation given the highly polymorphic nature of G-quadruplex structures and their respective structural flexibility. We specifically refrained from using longer homologues so as not to dissipate the perturbation induced by the *E–Z* transition into too many internal degrees of freedom.

Initial ^{1}H NMR (100 mM K^+) characterization of the short azobenzene-linked sequences chosen for this investigation showed signals in the imino region of the spectrum, typical for Hoogsteen-type hydrogen bonds (Figure 2b), suggesting the formation of G-quadruplex structures. Circular dichroism (CD) studies were performed to assess the conformational properties of the modified G-rich sequences. After the addition of 25 mM of K^+ ions, a positive signal around $\lambda =$ 295 nm and a negative signal near $\lambda = 260$ nm were detected for all three systems, indicating formation of antiparallel G-quadruplex structures (see Figure 3a for GG-**Az1**-GG and the Supporting Information for GG-**Az2**-GG and GG-**Az3**-GG).[33,34] Interestingly, ^{1}H NMR analysis of the different derivatives revealed structural polymorphism for GG-**Az2**-GG and GG-**Az3**-GG which was not detectable by CD. In all three cases, no formation of higher order aggregates was detected (see Figure S58 in the Supporting Information). For details on the thermal stability of the structures formed by the three sequences, please see Figure S5.

Only four ^{1}H NMR signals for imino groups, indicating a highly symmetric G-quadruplex structure, were detected after addition of K^+ to GG-**Az1**-GG. The ^{1}H NMR spectra of GG-**Az1**-GG also showed that at a K^+ ion concentration of 25 mM, the intensity of the set of imino signals was already 65% of its maximum value, whereas at a 5 mM K^+ ion concentration, the signal intensity was at 10% of its maximum (Figure 3b). In absence of K^+ ions there is no detectable interaction between the nucleobases, indicating that neither G-quadruplexes nor any other aggregates of the oligonucleotide strands are formed. Additionally, at Na^+ concentrations of up to 500 mM, we did not detect the formation of any secondary structure (Figures 3c and 3d). In this case, G-quadruplex formation was induced only after adding an additional 100 mM of K^+ ions (Figure 3d; Figure S39).

For another recent example of ion selectivity in G-quadruplexes and possible application in nanotechnology, see also Ref. [36]. Cation selectivity has also been reported for the thrombin-binding aptamer G-quadruplex,[37] whose G-tetrad core adopts the same folding topology as we have determined for GG-**Az1**-GG (see Figure 4 and the corresponding discussion). We propose that the smaller size of the Na^+ ion is not optimal to coordinate all eight O6 atoms in the two-tetrad cavity, which is necessary to keep the GG-**Az1**-GG in a stable quadruplex structure. Furthermore, the azobenzene linkers may introduce additional strain to the ionic channel, leading to the observed ion selectivity.

We investigated structural changes upon photoswitching of the azobenzene units. Two distinguishable sets of CD spectra could be obtained upon irradiation with either UV or visible light (Figure 3e). After an initial irradiation with UV light for 5 min, the CD signal at $\lambda = 295$ nm disappeared completely. Over the course of 30 min, the system reached thermal equilibrium (red data points in Figures 3e–g). Whereas the thermal *Z–E* isomerization occurs over the course of several days (Figure S42), irradiation with visible light for a short period of time (2 min) led to the almost complete recovery of the initial CD signal after 15 min of equilibration (Figure 3f) which could also be paralleled with corresponding NMR experiments (Figure 3h; Figure S60a). ^{1}H NMR spectroscopy showed the complete disappearance of signals for the imino protons upon irradiation with UV light and their almost complete recovery after irradiation with visible light (Figure 3i, 100 mM of K^+). We found that the degree of recovery after irradiation with visible light is a function of the DNA concentration: although at 50 μM the recovery of signals attributable to a G-quadruplex structure after irradiation with visible light is basically complete, a sample containing 125 μM DNA shows 75% recovery of resonance signals for the G-quadruplex 15 min after irradiation. However, the recovery of the G-quadruplex structure is complete after thermal equilibration (Figure S60a).

We speculate that at DNA concentrations concentrations greater than 50 μM, after UV illumination unspecific aggregates are formed (indicated by a broad signal in the aromatic region of the ^{1}H NMR spectrum) that slowly convert into the quadruplex folded state and/or to the completely unfolded state.

No effects of UV degradation (such as the photooxidation of guanine) were detected in the aromatic region of the 1D ^{1}H NMR spectra after repetitive UV/visible-light irradiation cycles (Figure S60b). Additionally, UV/Vis difference spectra (Figure S6) showed the differential absorption signature typical for G-quadruplexes.[38]

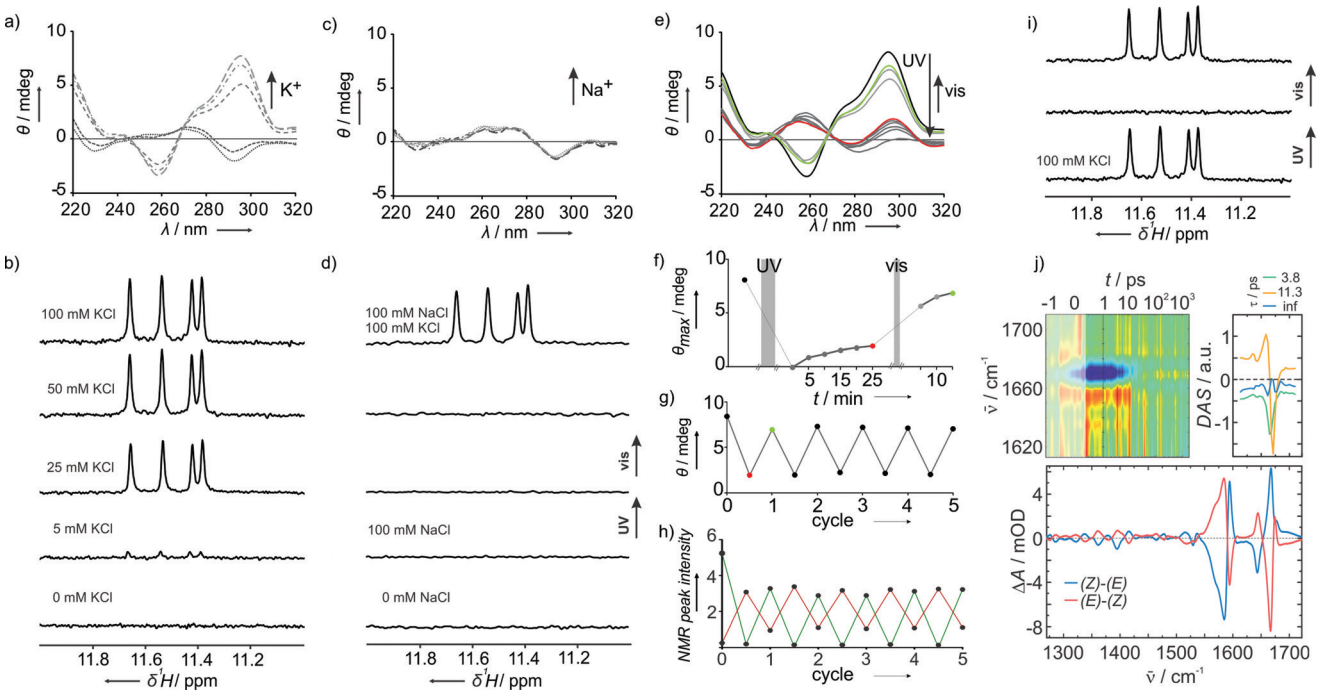

Figure 3. Spectroscopic characterization of the GG-**Az1**-GG sequence. a) CD spectra recorded with increasing K^+ concentrations (0, 5, 25, 50, 100 mM). b) 1D ^{1}H NMR spectra showing the imino region recorded in the presence of different KCl concentrations. c) CD spectra with increasing concentrations (0, 50, 100, 200, 300, 400, 500 mM) of Na^+. d) Imino region of the 1D ^{1}H NMR spectra in the presence of increasing amounts of NaCl and KCl. e) CD spectra of GG-**Az1**-GG with photoirradiation (5 min UV, 2 min visible light) and f) corresponding time course of the signal at $\lambda = 295$ nm under the indicated treatment. Cycling of the photoresponsive structural conversion of GG-**Az1**-GG by alternate irradiation with UV (15 min) and visible (4 min) light as monitored g) by CD at $\lambda = 295$ nm and h) by ^{1}H NMR ([DNA] = 125 μM, [KCl] = 100 mM) at $\delta = 11.55$ ppm (green line; monitoring the intensity of the signal for the imino proton of residue G5 in the *E* conformation) and at 6.64 ppm (red line; monitoring the intensity of the signal for the aromatic proton from the azobenzene moiety in the *Z* conformation). Absolute NMR peak intensities are referenced to an internal standard. i) Imino region of the 1D ^{1}H NMR spectra ([DNA] = 50 μM, [KCl] = 100 mM) showing spectral changes with photoirradiation (30 min UV, 2 min visible light). j) IR difference spectra (bottom); IR transient absorption data recorded from GG-**Az1**-GG after excitation of the azobenzene moiety at $\lambda = 335$ nm (top left); decay-associated spectra from the global lifetime analysis[35] of the transient absorption data (top right).

Photoswitching of GG-**Az1**-GG was also evident in the FTIR difference spectra (Figure 3j, bottom; Figure S53). The azobenzene isomerization and the subsequent disruption of the G-quadruplex structure led to a bathochromic shift (1675 $cm^{-1} \rightarrow 1667$ cm^{-1}) of the C=O stretching band[39–41] and to batho- and hypsochromic shifts of the bands associated with the C=C and C=N purine ring vibrations (1550–1590 cm^{-1} range),[39,41] features reported in the literature to be characteristic of G-quadruplex melting.[39,41] Ultrafast UV-pump/mid-IR-probe experiments[42] in the carbonyl stretching vibration range (Figure 3j, top left; Figure S54–55) were performed to investigate the dynamics of the G-quadruplex after *E* azobenzene excitation ($\lambda = 335$ nm). In the first picoseconds after laser excitation, the transient absorption data are dominated by the cooling dynamics of the C=O stretching band (1645–1680 cm^{-1}) with a lifetime of circa 11 ps. The absorption and bleach bands for the product state become visible after circa 10 ps (see the infinity spectrum in Figure 3j, top right). The last spectrum in the transient absorption data is essentially a *Z*–*E* IR spectrum of GG-**Az1**-GG at about 1800 ns. Evidently, this spectrum does not fully match the corresponding FTIR difference spectrum (Figure 3j, bottom), which indicates that despite the nearly instantaneous disruption of the FTIR features of a G-quadruplex, residual conformational dynamics occur on longer time scales.

For studies of GG-**Az1**-GG derivatives elongated or shortened at the 3′- and 5′-end and for the results obtained with the sequence GGG-**Az1**-GGG, please see Figures S40/S41 and S57, respectively.

To elucidate the molecular structure of the homogeneously folded GG-**Az1**-GG, 2D NMR experiments (2D ^{1}H–^{1}H NOESY, ^{1}H–^{13}C HSQC, and ^{1}H–^{13}C HMBC) were conducted to obtain the complete proton chemical shift assignment. Distance restraints were derived from NOE data and additional angular restraints were obtained from high-resolution ^{1}H–^{13}C HSQC, 2D ^{1}H–^{1}H P.E.COSY, and ^{1}H–^{31}P TOCSY experiments.[43] Assignment and *J*-coupling analysis are reported in the Supporting Information.

The folding topology of GG-**Az1**-GG was determined on the basis of NOESY data. As indicated by intra-tetrad H1–H8 connectivities (Figures S44), GG-**Az1**-GG adopts a symmetric, antiparallel G-quadruplex structure with tetrads composed as shown in Figure 4a,b. The edgewise loops containing the azobenzene moieties are located above the G2–G4 tetrad. The anomeric-aromatic region of the NOESY spectrum (Figure S45) indicated a *syn* conformation for the glycosidic bond of residues G1 and G4 and an *anti* conformation for residues G2 and G5.

Intriguingly, the structure of GG-**Az1**-GG resembles very much the ones of the G-quadruplex formed by the thrombin-binding aptamer (PDB: 148D, NMR; and PDB: 4DII, X-ray)[37,44] and in the promoter region of the B-raf gene (PDB: 4H29; see Figure S59 for an overlay).[45]

Hydrogen–deuterium exchange experiments (Figure S46) revealed that imino protons belonging to residues G1 and G5 are protected from solvent exchange. This result suggests a tetrameric G-quadruplex consisting of two dimeric units with the previously defined topology, in which the G1–G5 tetrads of both dimers face each other (Figure 4c). The stacking of two dimeric G-quadruplex units is supported by DOSY data (Figure S47). The structure of the tetramer (Figure 4d) was calculated using ARIA (details in the Supporting Information). The tetrameric arrangement was further supported by the fact that structure calculations as either monomer or dimer led to NOE violations. A significant number of NOEs are unambiguously assigned for the dimer and tetramer (Table 1). The prevalent conformation of the sugar moieties of G1, G2, and G4 is C2′-*endo* (confirmed by typical strong NOE cross-peaks and ^3J coupling constants). Only the 3′-terminal G5 sugar moiety is less well-defined, in part caused by resonance overlap, but manual inspection of the NOE cross-peaks (which are weaker than for the others) also suggest that this sugar possibly interconverts between the C3′-*endo* and C2′-*endo* conformations. Therefore no additional torsion angle restraints were included for the G5 nucleoside. The final bundle of structures was refined in explicit water, including three coordinated potassium ions within the tetrads. The structure is well-defined with an average root-mean-square deviation (RMSD) to mean for all atoms of 0.60 Å.

In summary, we have developed a photoswitchable G-quadruplex module and have characterized its photochemical behavior and its 3D conformation. Out of three investigated photoswitchable linkers in a number of sequence contexts, only GG-**Az1**-GG showed a defined and robust structural behavior. The system shows excellent photocontrol by UV/

Table 1: Statistics of the structure calculation.[a]

NOE distance restraints	**193**
Unambiguous NOEs:	146
intra-residue	87
sequential	42
long-range	1
dimer	4
tetramer	12
Ambiguous NOEs:	47
intra-residue	5
intra-monomer	22
monomer or dimer	7
monomer or tetramer	3
dimer or tetramer	8
mono-, di-, or tetramer	2
Distance restraints	**14**
intra-monomer hydrogen bonds	4
inter-monomer hydrogen bonds	4
potassium site coordination	6
Base planarity	**4**
intra-monomer	2
inter-monomer	2
Torsion angles	**35**
backbone	13
β (from ^3J(H5′$_{1,2}$,P))	3
glycosidic (χ)	4
sugar pucker	15
Violations	**0**
distances (>0.3 Å)	0
dihedral angles (>5°)	0
RMSD (average to mean)	
monomer (all atom)	0.55 Å
tetramer (all atom)	0.60 Å

[a] Statistics per monomer.

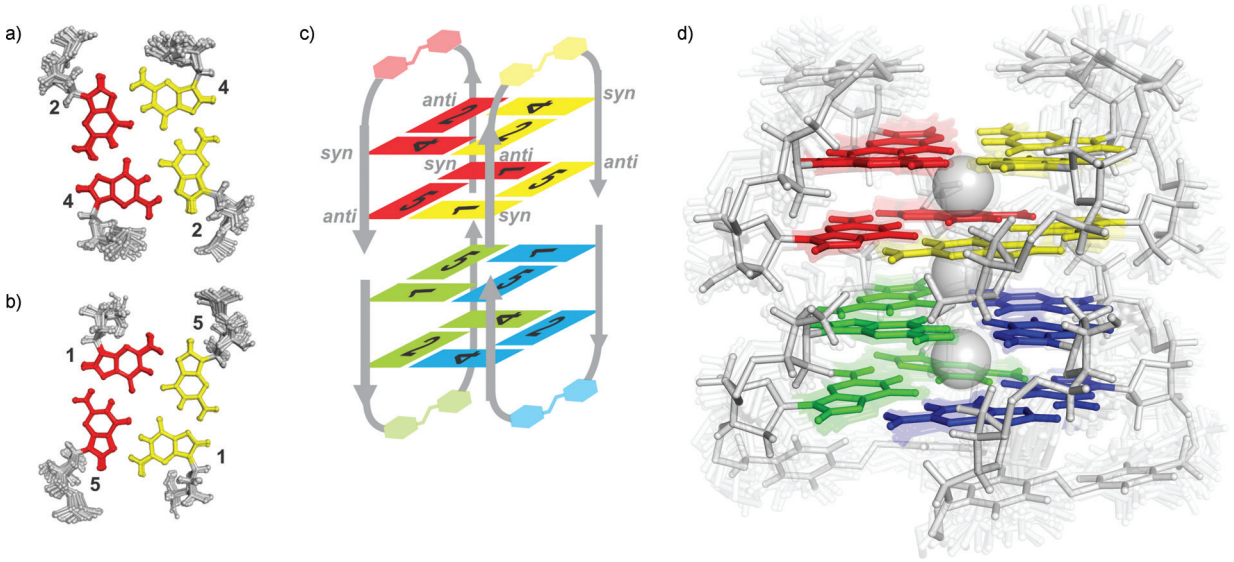

Figure 4. a) The G2–G4 tetrad and b) the G1–G5 tetrad with color coding corresponding both to the structure shown in (c) and to residue numbering given in Figure 1. c) Representation of the structure of the tetramer, with each monomer displayed in a different color. Conformations of the bases (*syn* or *anti*) are indicated. d) NMR solution structure of the G-quadruplex, showing the best representative of the bundle (indicated faintly in the background). K^+ ions are shown as gray spheres. PDB-code: 2N9Q; BMRB-code: 25915.

Vis irradiation, qualifying it as the smallest photocontrollable DNA switch reported to date. Irradiation with UV light of wavelength $\lambda = 365$ nm and with visible light is known not to be harmful to DNA or to cells and tissues.[17]

Numerous applications for such a photoswitchable G-quadruplex can be envisioned. The structure may, for example, find application as the glue for photocontrolled (dis)assembly of new fine-tunable nanoarchitectures or as an optomechanical molecular motor.[46]

Acknowledgements

The authors gratefully acknowledge help by Dr. Anna Lena Lieblein and funding by the Deutsche Forschungsgemeinschaft (DFG) in SFB902 and CLiC. J.W., H.S., and A.H. are members of the DFG-funded cluster of excellence: Macromolecular Complexes (EXC 115). Work in the group of H.S. has been funded by LOEWE project SynChemBio and by the state of Hesse (BMRZ). C.S. and J.W. acknowledge funding by the DFG (WA 1850/4-1).

Keywords: azobenzene · DNA structures · G-quadruplexes · IR spectroscopy · NMR spectroscopy

How to cite: *Angew. Chem. Int. Ed.* **2016**, *55*, 2738–2742
Angew. Chem. **2016**, *128*, 2788–2792

[1] T. Simonsson, *Biol. Chem.* **2001**, *382*, 621–628.
[2] S. Burge, G. N. Parkinson, P. Hazel, A. K. Todd, S. Neidle, *Nucleic Acids Res.* **2006**, *34*, 5402–5415.
[3] A. I. Karsisiotis, C. O'Kane, M. Webba da Silva, *Methods* **2013**, *64*, 28–35.
[4] I. Bessi, H. R. A. Jonker, C. Richter, H. Schwalbe, *Angew. Chem. Int. Ed.* **2015**, *54*, 8444–8448; *Angew. Chem.* **2015**, *127*, 8564–8568.
[5] D. Rhodes, H. J. Lipps, *Nucleic Acids Res.* **2015**, *43*, 8627–8637.
[6] G. Biffi, D. Tannahill, J. McCafferty, S. Balasubramanian, *Nat. Chem.* **2013**, *5*, 182–186.
[7] W. O. Tucker, K. T. Shum, J. A. Tanner, *Curr. Pharm. Des.* **2012**, *18*, 2014–2026.
[8] K. Y. Wang, S. McCurdy, R. G. Shea, S. Swaminathan, P. H. Bolton, *Biochemistry* **1993**, *32*, 1899–1904.
[9] E. A. Venczel, D. Sen, *J. Mol. Biol.* **1996**, *257*, 219–224.
[10] Z. Li, C. A. Mirkin, *J. Am. Chem. Soc.* **2005**, *127*, 11568–11569.
[11] M. Biyani, K. Nishigaki, *Gene* **2005**, *364*, 130–138.
[12] T. C. Marsh, J. Vesenka, E. Henderson, *Nucleic Acids Res.* **1995**, *23*, 696–700.
[13] D. P. N. Gonçalves, T. L. Schmidt, M. B. Koeppel, A. Heckel, *Small* **2010**, *6*, 1347–1352.
[14] F. Wang, X. Liu, I. Willner, *Angew. Chem. Int. Ed.* **2015**, *54*, 1098–1129; *Angew. Chem.* **2015**, *127*, 1112–1144.
[15] R. H. Kramer, D. L. Fortin, D. Trauner, *Curr. Opin. Neurobiol.* **2009**, *19*, 544–552.
[16] A. A. Beharry, G. A. Woolley, *Chem. Soc. Rev.* **2011**, *40*, 4422–4437.
[17] C. Brieke, F. Rohrbach, A. Gottschalk, G. Mayer, A. Heckel, *Angew. Chem. Int. Ed.* **2012**, *51*, 8446–8476; *Angew. Chem.* **2012**, *124*, 8572–8604.
[18] L. Wu, K. Koumoto, N. Sugimoto, *Chem. Commun.* **2009**, 1915–1917.
[19] F. Rohrbach, F. Schäfer, M. A. H. Fichte, F. Pfeiffer, J. Müller, B. Pötzsch, A. Heckel, G. Mayer, *Angew. Chem. Int. Ed.* **2013**, *52*, 11912–11915; *Angew. Chem.* **2013**, *125*, 12129–12132.
[20] F. Schäfer, J. Wagner, A. Knau, S. Dimmeler, A. Heckel, *Angew. Chem. Int. Ed.* **2013**, *52*, 13558–13561; *Angew. Chem.* **2013**, *125*, 13801–13805.
[21] G. Mayer, L. Kröck, V. Mikat, M. Engeser, A. Heckel, *ChemBioChem* **2005**, *6*, 1966–1970.
[22] A. Heckel, M. C. R. Buff, M. L. Raddatz, J. Müller, B. Pötzsch, G. Mayer, *Angew. Chem. Int. Ed.* **2006**, *45*, 6748–6750; *Angew. Chem.* **2006**, *118*, 6900–6902.
[23] T. L. Schmidt, M. B. Koeppel, J. Thevarpadam, D. P. N. Gonçalves, A. Heckel, *Small* **2011**, *7*, 2163–2167.
[24] H. Ito, X. Liang, H. Nishioka, H. Asanuma, *Org. Biomol. Chem.* **2010**, *8*, 5519–5524.
[25] H. Nishioka, X. Liang, T. Kato, H. Asanuma, *Angew. Chem. Int. Ed.* **2012**, *51*, 1165–1168; *Angew. Chem.* **2012**, *124*, 1191–1194.
[26] S. Ogasawara, M. Maeda, *Angew. Chem. Int. Ed.* **2009**, *48*, 6671–6674; *Angew. Chem.* **2009**, *121*, 6799–6802.
[27] S. Lena, P. Neviani, S. Masiero, S. Pieraccini, G. P. Spada, *Angew. Chem. Int. Ed.* **2010**, *49*, 3657–3660; *Angew. Chem.* **2010**, *122*, 3739–3742.
[28] D. P. N. Gonçalves, R. Rodriguez, S. Balasubramanian, J. K. M. Sanders, *Chem. Commun.* **2006**, 4685–4687.
[29] D. P. N. Gonçalves, S. Ladame, S. Balasubramanian, J. K. M. Sanders, *Org. Biomol. Chem.* **2006**, *4*, 3337–3342.
[30] R. Rodriguez, G. D. Pantoş, D. P. N. Gonçalves, J. K. M. Sanders, S. Balasubramanian, *Angew. Chem. Int. Ed.* **2007**, *46*, 5405–5407; *Angew. Chem.* **2007**, *119*, 5501–5503.
[31] X. Wang, J. Huang, Y. Zhou, S. Yan, X. Weng, X. Wu, M. Deng, X. Zhou, *Angew. Chem. Int. Ed.* **2010**, *49*, 5305–5309; *Angew. Chem.* **2010**, *122*, 5433–5437.
[32] Y. Kim, J. A. Phillips, H. Liu, H. Kang, W. Tan, *Proc. Natl. Acad. Sci. USA* **2009**, *106*, 6489–6494.
[33] S. Paramasivan, I. Rujan, P. H. Bolton, *Methods* **2007**, *43*, 324–331.
[34] A. Randazzo, G. P. Spada, M. Webba da Silva, *Top. Curr. Chem.* **2012**, *330*, 67–86.
[35] C. Slavov, H. Hartmann, J. Wachtveitl, *Anal. Chem.* **2015**, *87*, 2328–2336.
[36] L. Olejko, P. J. Cywinski, I. Bald, *Angew. Chem. Int. Ed.* **2015**, *54*, 673–677; *Angew. Chem.* **2015**, *127*, 683–687.
[37] I. Russo Krauss, A. Merlino, A. Randazzo, E. Novellino, L. Mazzarella, F. Sica, *Nucleic Acids Res.* **2012**, *40*, 8119–8128.
[38] J.-L. Mergny, J. Li, L. Lacroix, S. Amrane, J. B. Chaires, *Nucleic Acids Res.* **2005**, *33*, e138.
[39] H. T. Miles, J. Frazier, *Biochem. Biophys. Res. Commun.* **1972**, *49*, 199–204.
[40] M. R. Guzmán, J. Liquier, S. K. Brahmachari, E. Taillandier, *Spectrochim. Acta Part A* **2006**, *64*, 495–503.
[41] J. A. Walmsley, M. L. Schneider, P. J. Farmer, J. R. Cave, C. R. Toth, R. M. Wilson, *J. Biomol. Struct. Dyn.* **1992**, *10*, 619–638.
[42] K. Neumann, M.-K. Verhoefen, I. Weber, C. Glaubitz, J. Wachtveitl, *Biophys. J.* **2008**, *94*, 4796–4807.
[43] H. Schwalbe, J. P. Marino, G. C. King, R. Wechselberger, W. Bermel, C. Griesinger, *J. Biomol. NMR* **1994**, *4*, 631–644.
[44] P. Schultze, R. F. Macaya, J. Feigon, *J. Mol. Biol.* **1994**, *235*, 1532–1547.
[45] D. Wei, A. K. Todd, M. Zloh, M. Gunaratnam, G. N. Parkinson, S. Neidle, *J. Am. Chem. Soc.* **2013**, *135*, 19319–19329.
[46] M. McCullagh, I. Franco, M. A. Ratner, G. C. Schatz, *J. Am. Chem. Soc.* **2011**, *133*, 3452–3459.

Received: November 4, 2015
Revised: December 11, 2015
Published online: January 25, 2016

